STRESS-STRAIN PROPERTIES OF HSS STEEL WELDED JOINT HETEROGENEOUS STRUCTURE: EXPERIMENTAL AND NUMERICAL EVALUATION

D. TOMERLIN*[1], D. KOZAK**, N. GUBELJAK***,
M. MAGIĆ KUKULJ*

**DOK-ING Ltd., HR-10000, Zagreb, Croatia*
***Mechanical Engineering Faculty, University of Slavonski Brod, HR-35000, Slavonski Brod, Croatia*
****Faculty of Mechanical Engineering, University of Maribor, SI-2000, Maribor, Slovenia*
[1]corresponding author

DOI 10.3217/978-3-85125-968-1-23

ABSTRACT

Welded joints show significant heterogeneity as they are composed of base metal, heat affected zone and weld metal. Heat Affected Zone (HAZ) is further divided into characteristic segments. All the listed zones of the welded joints have certain microstructural differences and consequent differences in mechanical properties. Mechanical experimental examination and determination of stress-strain characteristics of such heterogeneous welded joints structure, especially in certain segments of the HAZ is very difficult. The classical approach to stress-strain testing using standard tensile specimens have only limited applicability, as even the subsize tensile specimens are difficult to position within the narrow HAZ segments. Difficulties in such experimental measurements and the possibility of testing the welded joints in full scope are the motivation for use of alternative experimental methods. The paper considers double-V butt joint made of High Strength Steel (HSS), welded with filler metal having approximately the same mechanical properties as base metal. Experimental work is focused on stress-strain properties determination with Mini tensile Specimens (MTS) used to determine the properties along the transverse weld line. The aim of the paper is the development of an appropriate computer model based on sufficient experimental data, describing the complete welded joint and its specific zones. The evolution of such model is done, starting with a simple model and refining it to a complex, fully segmented welded joint model. This final welded joint model is implemented into ASTM E8 large size specimen, oriented transverse to the welded joint, and covering all specific zones of the welded joint. Material behaviour is simulated using the ductile damage initiation criterion. Tensile test simulation results show good correlation between experimental data and numerical evaluation. Simulated tensile specimen fracture location matches the HAZ segment with decreased strength values, most prone to failure. The paper demonstrates the possibility of experimental determination of stress-strain mechanical properties throughout the heterogeneous welded joint regions, using the MTS specimens. These results can then be used to create a fully segmented welded joint model for tensile testing, or some similar applications.

Keywords: Stress-strain, welded joint heterogeneity, high strength steel, experimental methods, numerical analysis

INTRODUCTION

In scope of fusion welded joint, several characteristic zones can be observed: base metal (BM), weld metal (WM) and heat affected zone (HAZ). HAZ refers to part of the base metal which has not undergone the melting process during the fusion welding, rather it was heated to an elevated temperature below the melting point, and subsequently cooled. Width of HAZ strongly depends on chosen welding process, welding parameters, heat input, welded joint geometry, number of passes etc. [1, 2]. The HAZ can be further divided into several characteristic segments with different microstructures and mechanical properties. In the past studies, significant research of fusion weld characteristic zones is already done [3-5]. When choosing the filler material in relation to base metal, the discrepancy between WM and BM mechanical properties is described by "weld strength mis-match" [6, 7].

In scope of overall welded joint, HAZ is most failure prone zone during service life. Because of this it is of great importance to control the overall welding process parameters in order to maintain HAZ width and its mechanical properties within tolerable limit. Heterogeneity is indicative throughout the welded joint, and can be observed in the microstructural and mechanical properties variations.

Experimental investigations of high strength steel welded joints properties, as well as correlated numerical simulations, have previously been conducted by various researchers [8-12]. Investigations presented in scope of this paper are aimed to give deeper insights into mechanical properties of heterogeneous welded joint made from high strength steel, with emphasis on stress-strain behaviour.

The challenge of finding the suitable experimental method for determination of stress-strain characteristics of heterogeneous welded joints structure, is addressed by the authors. General issues relate to the selection of suitable experimental specimens that are able to describe mechanical properties of welded joint and certain segments of the HAZ [13-16]. Since such specimens must be of subsize dimensions, the problems of their manufacture also occur consequently. Some of the experimental methods that can be applied are:

- ASTM E8 tensile subsize specimens for determination of welded joint properties on general scale.
- Mini Tensile Specimens (MTS) for determination of stress-strain properties along the transverse weld line [6].
- Profilometry-based Indentation Plastometry (PIP) method for detailed stress-strain measurement on small surface area using the special indenter equipment [17-19].

In scope of this paper, MTS specimen method is used to determine the stress-strain behaviour of heterogeneous welded joint structure. The test coupon of 40mm thick rolled plates is welded using double-V butt joint. Transverse section cut is done, and complete subsection volume for MTS specimens extracted. Shown in Fig. 1.

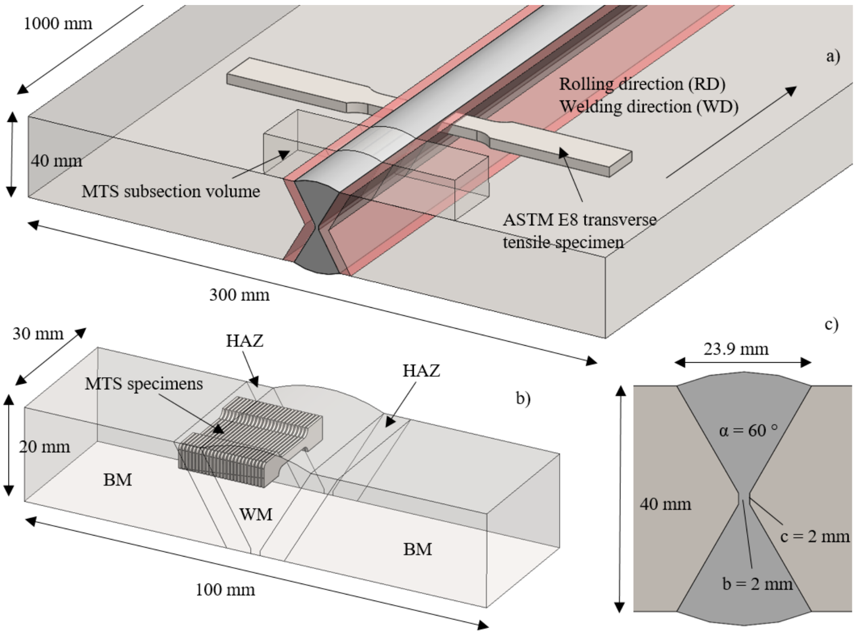

Fig. 1 Experimental methods for determination of stress-strain characteristics of heterogeneous welded joint structure: (a) welded test coupon, (b) MTS subsection volume with specimens and (c) X joint preparation and dimensions

Detailed characterization of mechanical properties throughout the heterogeneous welded joint is extremely important for the development of a realistic welded joint model and the implementation of numerical analysis. Several welded joint models are created, starting with a simple model and refining it to a complex, fully segmented welded joint model. Modelling of such a complex joint, and simulating its material behaviour, is made possible by using the MTS method experimentally collected material data.

Validation of segmented welded joint model is done based on the uniaxial tensile test, using the ASTM E8 large size flat specimen, oriented transverse to the welded joint, and covering all the specific zones, Fig.1. Ductile damage initiation criterion, integrated into ABAQUS software, is used to simulate response during the tensile test. Numerical simulation is giving the accurate insight into stress-strain behavior, while predicting the specimen damage evolution and final fracture location. Good correlation between experimental stress-strain and simulation results can be observed [20-25].

MATERIALS AND EXPERIMENTAL METHODS

MATERIALS AND WELDED JOINT

The paper considers double-V butt joint (X joint) made of High Strength Steel (HSS), welded with filler metal having the mechanical properties selected according to base metal. The HSS base metal (BM) is S690QL1 fine-grained steel for structural applications, manufactured by quenching and tempering (QT) process, with declared yield strength $R_{p0.2} \geq 690$ MPa. Weld metal (WM) inside the joint is Mn3Ni1CrMo (ER110S-G) and is deposited using the gas metal arc welding (GMAW) process with 1.2mm diameter filler wire. WM declared yield strength is $R_{p0.2} \approx 800$ MPa.

Weld strength mismatch is determined using the equation:

$$M = \frac{\sigma_{\mathrm{YW}}}{\sigma_{\mathrm{YB}}} \tag{1}$$

where σ_{YW} and σ_{YB} represent the yield strength of the weld metal (WM) and the yield strength of the base metal (BM), respectively. In this welded joint, mismatch factor M = 1.16 which indicates the slightly over-matching (OM) weld metal [6, 7].

The BM plates used in X welded joint are of 40 mm thickness. The joint is welded using multiple passes as shown in Fig. 2. Process parameters are given in Table 1.

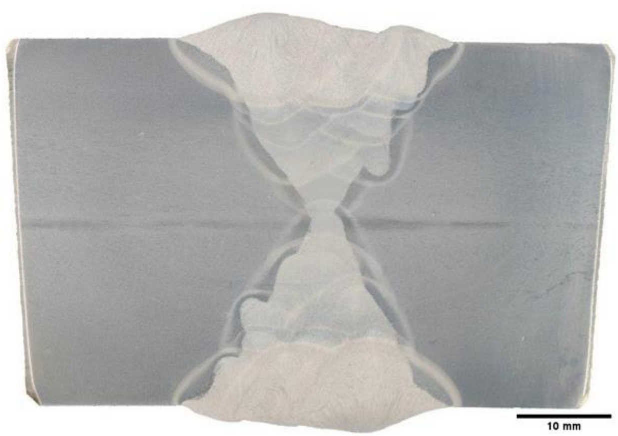

Fig. 2 X welded joint

Table 1 Welding process parameters

Pass no.	Location	I [A]	U [V]	v_w [cm/min]	η	Q [kJ/mm]
1-3	root	195	26	28.5	0.8	0.85
4-22	fill + cover	280	29	45	0.8	0.87

MTS TESTING

The tensile properties along the transverse welded joint line are obtained using the set of Mini Tensile Specimens (MTS) [6]. These are basically flat sheet specimens, with specific dimensions L = 24 mm, A = 9 mm, B = 6 mm, C = 5 mm, and thickness T = 0.5 mm, geometry is shown in Fig. 4. MTS are positioned in filler pass zone (MTS R1-24 and R25 at centerline) of X welded joint. Set is placed in transverse direction including BM, HAZ, and WM up to joint centerline, as shown in Fig. 1 and Fig. 3. MTS are manufactured using the Electrical Discharge Wire Cutting (EDWC) technology, with the wire diameter 0.25 mm, which also dictates the lateral distance between the test specimens.

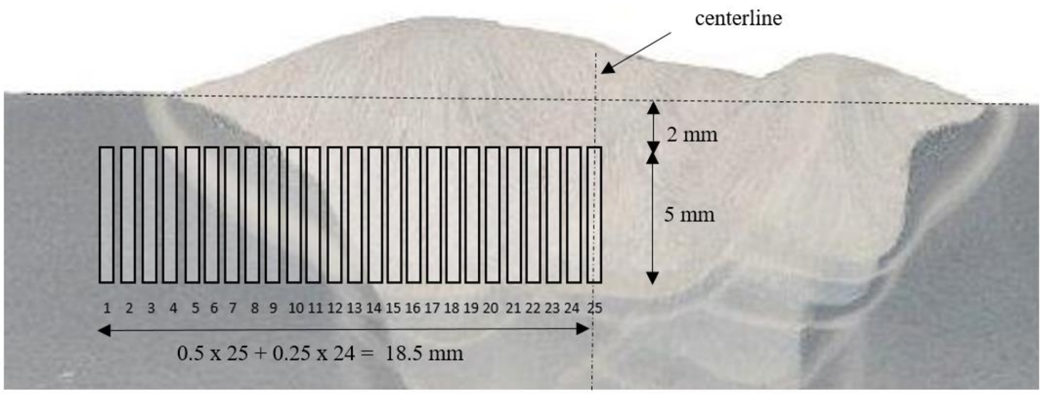

Fig. 3 MTS specimens positioning along the welded joint

Using MTS specimens experimental testing method, it is possible to gain deeper insight into tensile properties of welded joint characteristic zones, as well as specific HAZ segments. Observing the specific locations from which the individual MTS specimens were extracted, a rough division can be made along the welded joint transverse line, according to characteristic zones:

- MTS R1 - MTS R5 (BM)
- MTS R6 - MTS R13 (HAZ)
- MTS R14 - MTS R25 (WM)

Engineering stress-strain curves obtained from MTS tensile tests are given in Fig. 4. It can be observed that the strength values are following an increasing trend from BM to WM. In HAZ zone, there is the continuity interruption, with peak values in locations MTS R11 - R13.

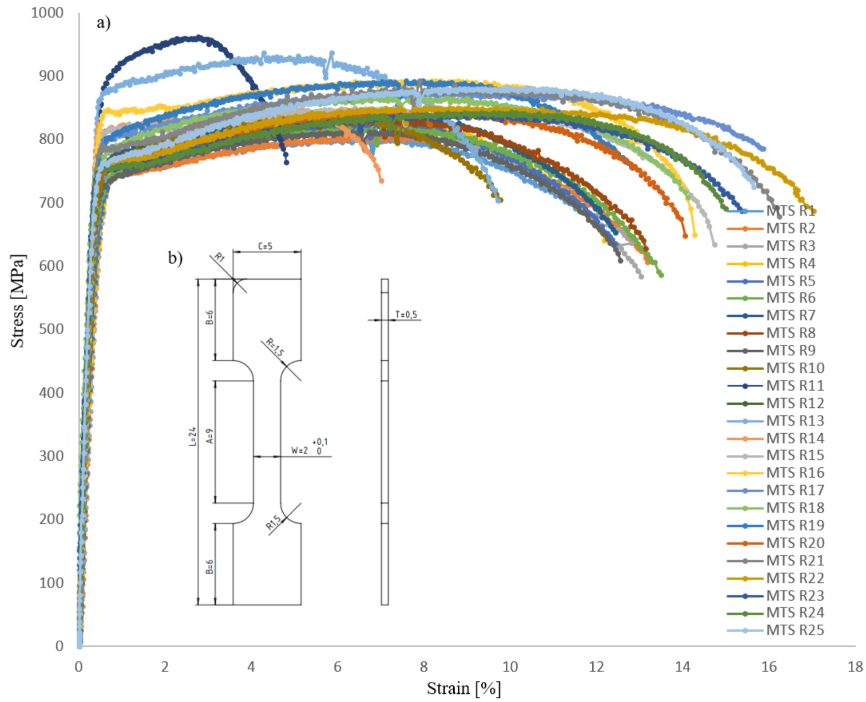

Fig. 4 MTS specimens tensile testing: (a) engineering stress-strain curves and (b) MTS specimen dimensions

Local mechanical properties, along the transverse welded joint line, are shown in Fig.5.

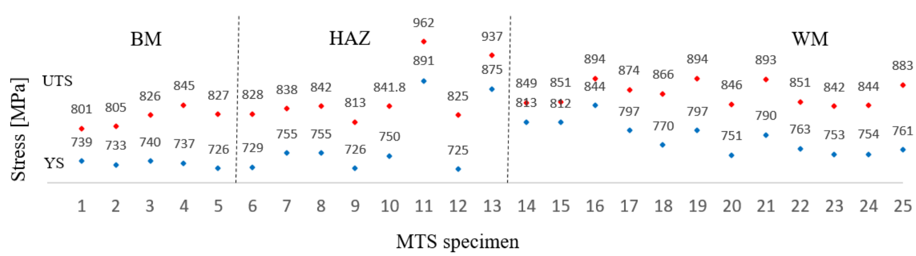

Fig. 5 Tensile properties along the transverse welded joint line

NUMERICAL MODELLING

DUCTILE DAMAGE

In order to describe the behaviour of elasto-plastic metallic materials, taking into account progressive damage material degradation up to failure, ductile damage model is used. The ductile damage initiation criterion is model for predicting the onset of damage due to nucleation, growth, and coalescence of voids. The typical tensile test stress-strain curve, with progressive damage degradation is shown in Fig. 6. Initial curve partition (0a) is linear-elastic part. Past the yield stress σ_0, in curve partition (ab), the material undergoes stable plastic deformation with strain hardening effect. The point *b* is the initiation threshold of plastic instability, with damage parameter $D = 0$. In the failure partition (bd) stiffness degradation and damage evolution is present. At point d damage parameter $D = 1$, and crack initiates as an indication of failure. [20].

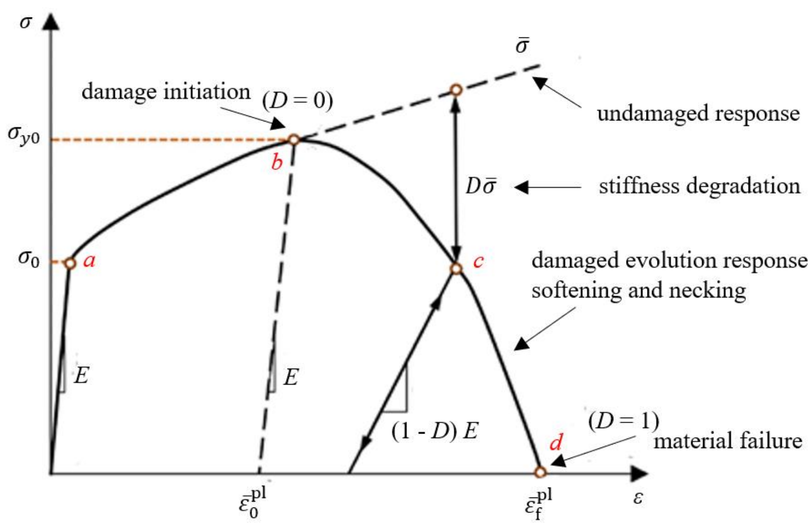

Fig. 6 Stress-strain curve with progressive damage degradation

The damage parameter *D*, governing the failure model, is defined by the equation:

$$D = \sum \frac{\bar{\varepsilon}^{\mathrm{pl}}}{\bar{\varepsilon}_{\mathrm{f}}^{\mathrm{pl}}} \leq 1 \tag{2}$$

where $\bar{\varepsilon}^{\mathrm{pl}}$ is equivalent plastic strain, and $\bar{\varepsilon}_{\mathrm{f}}^{\mathrm{pl}}$ is plastic strain at failure. Damage parameter *D* is changing from 0 (non-damaged) to 1 (material failure). At arbitrary time increment in the analysis, the damaged stress state is given by the scalar damage equation:

$$\sigma_D = (1 - D)\bar{\sigma} \tag{3}$$

where $\bar{\sigma}$ is the effective (undamaged) stress calculated in the current increment. For the ductile damage initiation, the model assumes that the equivalent plastic strain at the damage onset $\bar{\varepsilon}_{\mathrm{D}}^{\mathrm{pl}}$ is function of stress triaxiality η and equivalent plastic strain rate $\dot{\bar{\varepsilon}}^{\mathrm{pl}}$:

$$\bar{\varepsilon}_{\mathrm{D}}^{\mathrm{pl}}\left(\eta, \dot{\bar{\varepsilon}}^{\mathrm{pl}}\right) \tag{4}$$

Damage evolution defines the post damage-initiation material behavior. The equivalent plastic displacement $\bar{u}^{\mathrm{pl}}$, after damage initiation, is defined according to equation:

$$\dot{\bar{u}}^{\mathrm{pl}} = L\dot{\bar{\varepsilon}}^{\mathrm{pl}} \tag{5}$$

where L is the characteristic mesh element length. Parameter $\bar{u}_{\mathrm{f}}^{\mathrm{pl}}$ relates to elongation of the element from damage initiation to failure. Severely damaged elements, reaching the maximum degradation limit, are deleted from the model thus achieving the specimen geometry separation. Assuming the constant stress triaxiality and strain rate, material damage behavior is strongly dependant on damage initiation fracture strain $\bar{\varepsilon}_{\mathrm{D}}^{\mathrm{pl}}$ parameter and damage evolution displacement at failure $\bar{u}_{\mathrm{f}}^{\mathrm{pl}}$ parameter [20-25]. The comparison of several Ductile Damage Models (DDM) is shown in Fig. 7, with parameters given in Table 2.

Table 2 Ductile Damage Models parameters

Model	L [mm]	$\bar{\varepsilon}_{\mathrm{D}}^{\mathrm{pl}}$	$\bar{u}_{\mathrm{f}}^{\mathrm{pl}}$ [mm]
DDM 1	0.5	0.08	0.005
DDM 2	0.5	0.08	0.1
DDM 3	0.5	0.20	0.005
DDM 4	0.5	0.20	0.1

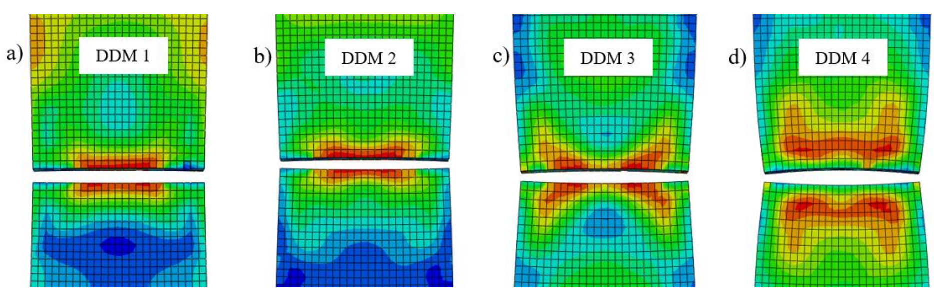

Fig. 7 Fracture surfaces of tensile specimens: (a) DDM 1, (b) DDM 2, (c) DDM 3 and (d) DDM 4

It can be observed that increase in fracture strain value leads to fracture ductility with more prominent necking effect, and increased concavity of the fracture surface. Displacement at failure affects the element elongation from damage initiation to failure.

WELDED JOINT - MODEL EVOLUTION

The purpose of welded joint model is to describe the overall weld behaviour in scope of numerical simulations application. Due to the existence of heterogeneity, localization of mechanical properties is extremely important for the development of a realistic welded joint model. The authors have investigated several Welded Joint Models (WJM) gradually upgrading them according to the degree of complexity, shown in Fig. 8.

WJM 1 is basic model that includes BM + WM + BM zones. Construction of this model requires material properties only on general scale that can be obtained using the standard size specimens located in BM and All-Weld Metal (AWM). Depending on the mismatch of material properties, fracture will occur either in BM or WM.

WJM 2 is an upgraded model that includes BM + HAZ + WM + HAZ + BM zones. General material properties of HAZ zone need to be determined, and ASTM E8 tensile subsize specimens are suitable for this purpose, Fig. 1. Considering the mechanical properties, and material mismatch, failure will occur in the weakest zone.

WJM 3 is the final, most complex, fully segmented model that includes BM + HAZ + WM + HAZ + BM zones (24 + 1 + 24 = 49 segments). Using the MTS method, material properties are determined for specific segments, and corresponding model is constructed. Failure can be precisely located in most damage prone segment. This model is an improvement against the earlier status, giving more accurate predictions.

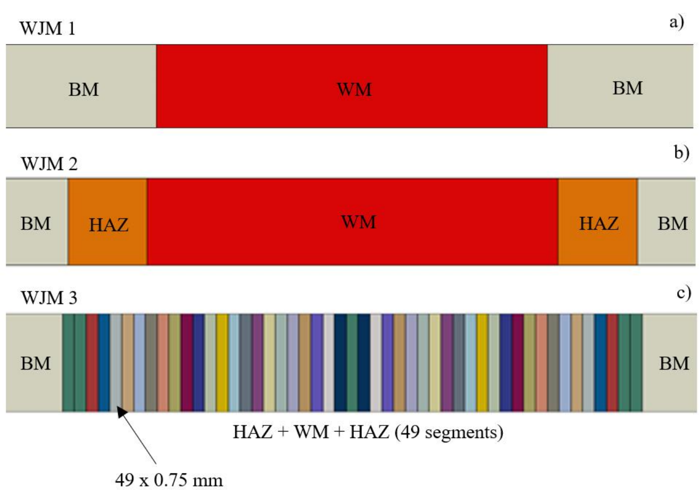

Fig. 8 Welded Joint Models (WDM) evolution: (a) WJM 1 basic, (b) WJM 2 upgraded and (c) WJM 3 segmented model

RESULTS AND DISCUSSION

TENSILE TESTING SIMULATION

Finite element analysis of all tensile tests in scope of this work is done using the ABAQUS/Explicit. ASTM E8 tensile large size flat sheet specimens positioned in transverse direction to welded joint is modelled. Their dimensions are L = 200 mm, A = 57 mm, B = 62.6 mm, C = 20 mm, W = 12.5 mm, and thickness T = 5 mm. Specimens are meshed using the hexahedral C3D8 element. Fine mesh is used in the whole reduced section volume (A x W x T), with characteristic element length of L = 0.5 mm. Selected mesh element size is in accordance with previous study done by Yan et al. indicating that 0.5 mm element could not affect the accuracy of fracture simulation [22]. Bottom grip section of specimen is fully clamped, while top grip section is subjected to displacement, simulating the tensile loading conditions, Fig. 9.

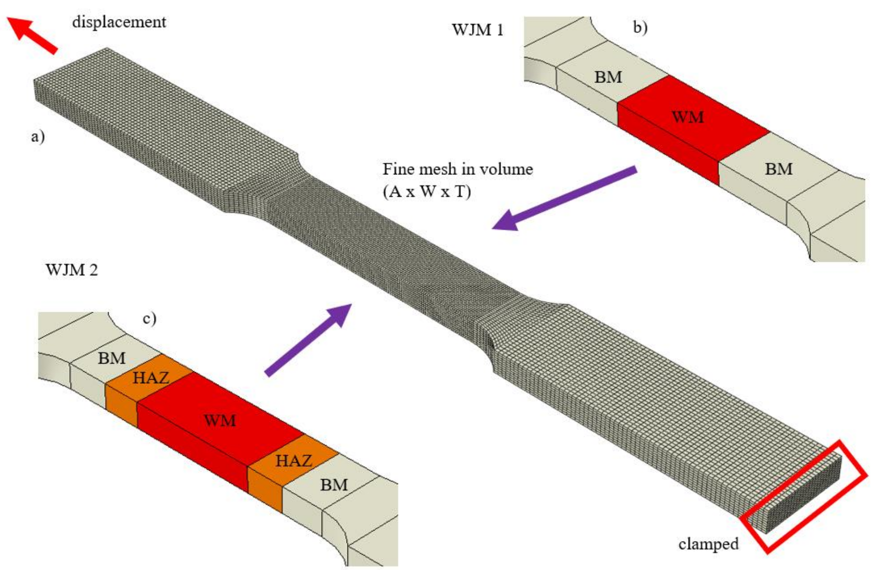

Fig. 9 Tensile flat sheet specimen ASTM E8 (a) FE model, (b) WJM 1 and (c) WJM 2 model

Initial considerations and simulations address models WJM 1 and WJM 2 based on the material properties on general scale, with fundamental welded joint heterogeneity taken into consideration. Simulations were carried out with the purpose of determining the location of tensile specimen breakage due to the various combinations of welded joint material properties mismatch. Material properties can be either under-matched (UM) or over-matched (OM), while matched properties are not considered here and thus simulated. Based on the results of ASTM E8 tensile subsize specimens testing for determination of welded joint properties on general scale, four steel materials are identified and implemented into models. Their strength and damage parameters are given in Table 3.

Table 3 Strength and damage properties from ASTM E8 tensile testing on general scale

Material	$R_{p0.2}$ [MPa]	R_m [MPa]	$\bar{\varepsilon}_D^{pl}$	$\bar{u}_f^{pl}$ [mm]
Steel 1	760	810	0.2	0.05
Steel 2	780	835	0.09	0.005
Steel 3	785	840	0.12	0.02
Steel 4	800	860	0.18	0.01

The comparison of several WJM 1 and WJM 2 models with strength mismatch and damage variations is shown in Fig. 10, with material variations and mismatch factors *M* given in Table 4.

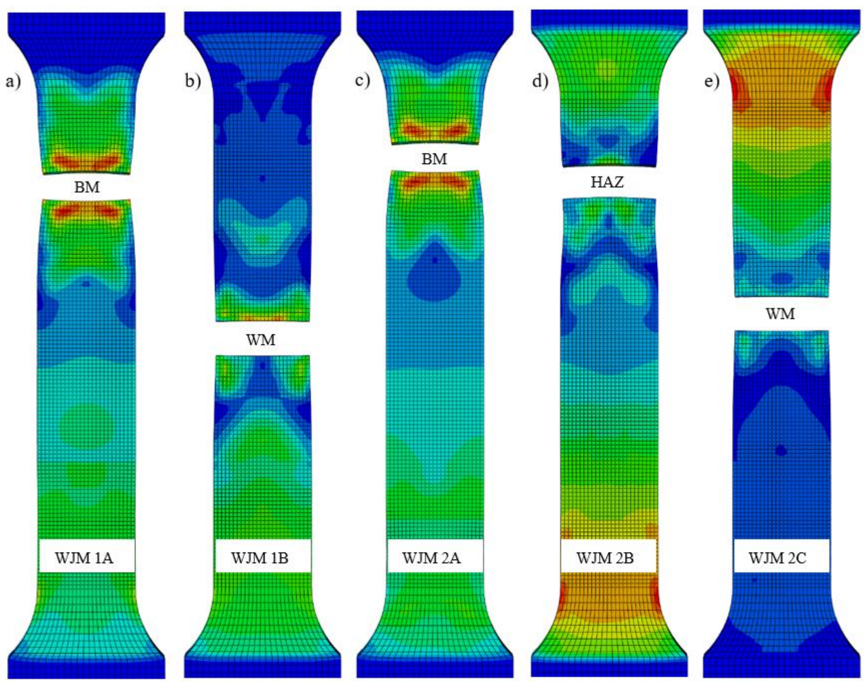

Fig. 10 Fracture locations for WJM 1 and WJM 2 models, based on material properties mismatch

Table 4 Mismatch material variations for WJM 1 and WJM 2 models

Model	BM	WM	HAZ	*M*
WJM 1 A	Steel 1	Steel 4	-	1.053 (OM)
WJM 1 B	Steel 4	Steel 2	-	0.975 (UM)
WJM 2 A	Steel 1	Steel 4	Steel 2	1.053 (OM)
WJM 2 B	Steel 2	Steel 4	Steel 1	1.026 (OM)
WJM 2 C	Steel 4	Steel 2	Steel 3	0.975 (UM)

It can be observed that fracture of all simulated samples occurs in the material region with the lowest strength, corresponding to Steel 1 or 2 material. Using te WJM 1 and WJM 2 models, with known strength data of individual zones of the material, even at a general level, predictions of the critical locations where breakage will occur can be simulated. Damage parameters define the fracture geometry and evolution, as depicted by DDM models.

After performing analyzes of simple models WJM 1 and WJM 2, the fully segmented welded joint model WJM 3, which describes the welded joint heterogeneity in detail, is integrated into tensile specimen model. Same tensile specimen geometry per ASTM E8 as well as numerical modeling preparation and conditions are applied. Purpose of this model is to accurately represent the real damage response, therefore previously determined material properties from MTS testing are used. Elastic modulus is experimentally determined for each of the 25 material segments, while Poisson's ratio of 0.3 is used. Tensile specimen with WJM 3 is shown in Fig. 11.

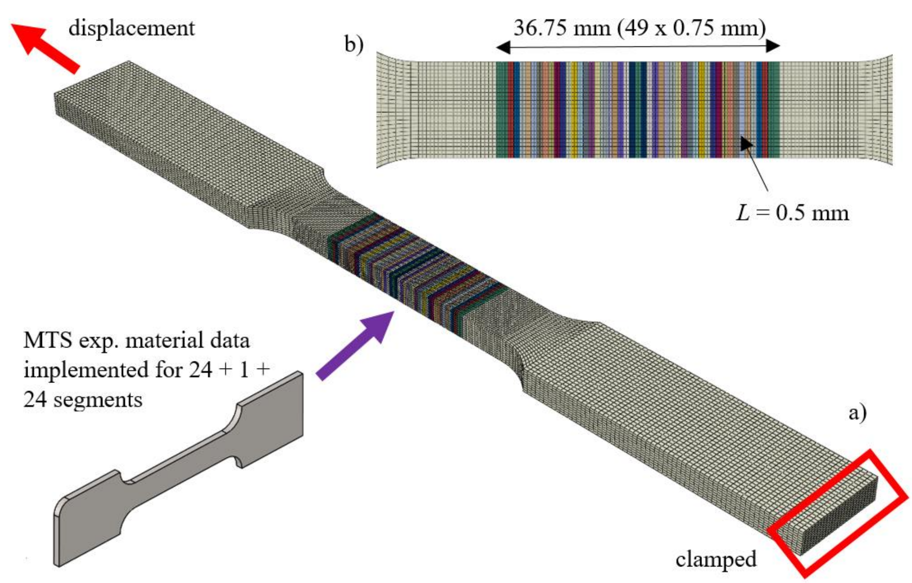

Fig. 11 Tensile specimen WJM 3 (a) FE model and (b) fully segmented welded joint model

a)

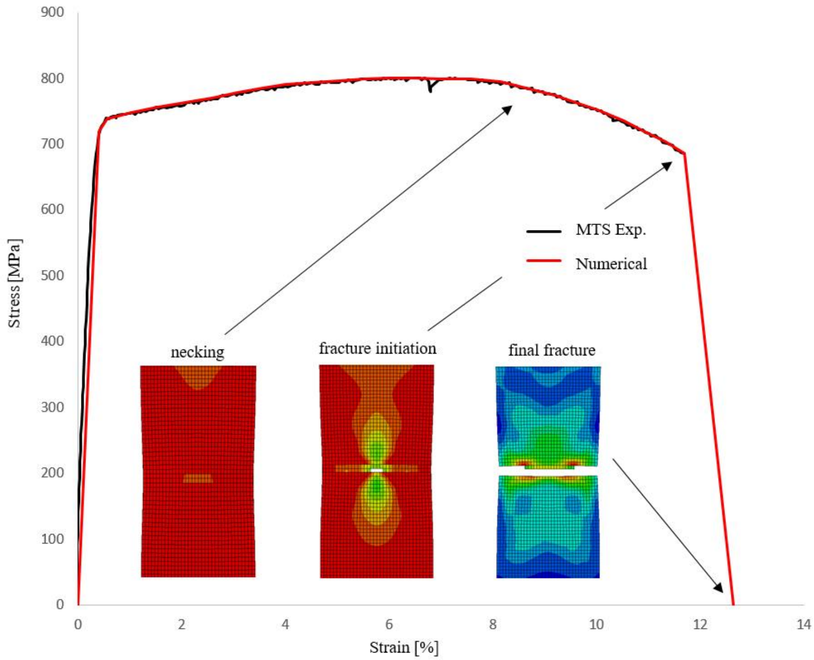

b)

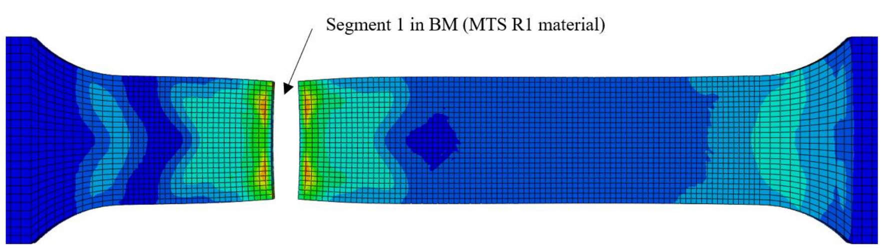

Fig. 12 Tensile testing FE analysis using WJM 3 model (a) stress-strain diagram and (b) specimen fracture location

WJM 3 tensile specimen failed in segment with lowest UTS value, corresponding to MTS R1 located in the BM zone. This is in an agreement with slightly over-matching WM, and local strength variations in BM. Stress-strain curve from FE analysis is compared with experimental curve for MTS R1 specimen. Good correlation can be observed, Fig. 12. Ductile damage parameters for MTS R1 specimen material are given in Table 5. It can be concluded that this damage model has the most similarities with DDM2 model, resulting in similar necking behavior and fracture surface appearance, Table 2 and Fig. 7.

Observing the numerically simulated damage behaviour of tensile specimen, initiation of ductile fracture is located at the central position of the necking region, which is generally expected during the experimental tensile testing. Tensile specimen behaviour is simulated and the corresponding steps are shown in Fig. 12.

Table 5 Ductile Damage parameters for transverse tensile testing of WJM 3 model

Model	***L* [mm]**	$\bar{\varepsilon}_{\mathrm{D}}^{\mathrm{pl}}$	$\bar{u}_{\mathrm{f}}^{\mathrm{pl}}$ **[mm]**
MTS R1	0.5	0.065	0.068

CONCLUSION

The paper addresses the heterogeneity of welded joint made of HSS steel, using experimental methods and proposing a model for application in computer simulations. The primary conclusions are as follows:

- Detailed characterization of mechanical properties throughout the heterogeneous welded joint is extremely important for the development of a realistic welded joint model. Material properties in narrow segments can be determined using the MTS experimental method.
- Simple WJM 1 and WJM 2 models enable predictions of the critical locations in scope of welded joint where breakage will occur.
- Evolution of welded joint models is done in order to build a model suitable for describing the heterogeneity of the welded joint. Finally, WJM 3 fully segmented model is proposed.
- Tensile testing FEM damage simulation shows the ability of welded joint model to replicate the experimental response. Model is able to predict the exact fracture location.
- Segmented welded joint model has potential for similar applications where it is necessary to describe the heterogeneity of the welded joint.

ACKNOWLEDGEMENTS

This work has been supported by Slovenian research agency ARRS for part of the research supported by Program P2-0137 “Numerical and Experimental Analysis of Nonlinear Mechanical Systems” and DOK-ING Ltd., Zagreb, Croatia, providing the research material, and funding the test specimens preparation and associated works.

References

[1] K. E. EASTERLING: *Introduction to the Physical Metallurgy of Welding*, Second Edition, London, Butterworth-Heinemann, 1992.
[2] S. KOU: *Welding Metallurgy*, Second Edition, John Wiley and Sons, Hoboken, New Jersey, 2003.
[3] E.F. NIPPES: ‘The weld heat-affected zone’, *Weld J*, 38 (1), pp. 1-17, 1959.
[4] W.F. SAVAGE, E.F. NIPPES, E.S. SZEKERES: ‘A Study of Weld Interface Phenomena in a Low Alloy Steel’, *Weld J*, 55 (9), pp. 260-268, 1976.
[5] O.M. AKSELSEN, G. RØRVIK,, M.I. ONSØIEN, Ø. GRONG: ‘Assessment and Predictions of HAZ Tensile Properties of High-Strength Steels’, *Weld J*, 68 (9), pp. 356-362, 1989.

[6] L. STARČEVIĆ, N. GUBELJAK, J. PREDAN: 'The Numerical Modelling Approach with a Random Distribution of Mechanical Properties for a Mismatched Weld', *Materials,* 14, 5896, https://doi.org/10.3390/ma14195896.

[7] P. KONJATIĆ, M. KATINIĆ, D. KOZAK, N. GUBELJAK: 'Yield Load Solutions for SE(B) Fracture
Toughness Specimen with I-Shaped Heterogeneous Weld', *Materials,* 15, 214, https://doi.org/10.3390/ma15010214.

[8] D. TOMERLIN, D. KOZAK, N. GUBELJAK, D. DAMJANOVIĆ: 'Numerička analiza distorzija i zaostalih naprezanja pri zavarivanju kutnih spojeva S690QL limova', *10. Susret HDM,* 01. i 02. listopada, Slavonski Brod, 2020.

[9] H. ISMAR, Z. BURZIC, N.J. KAPOR, T. KOKELJ: 'Experimental Investigation of High-Strength Structural Steel Welds', *Journal of Mechanical Engineering*, 58, 6, pp. 422-428, 2012, DOI:10.5545/sv-jme.2011.281

[10] E. CADONI, D. FORNI: 'Strain-rate effects on S690QL high strength steel under tensile loading', *Journal of Constructional Steel Research*, volume 175, 106348, 2020, https://doi.org/10.1016/j.jcsr.2020.106348.

[11] M. GÁSPÁR, D. FORNI: 'Effect of Welding Heat Input on Simulated HAZ Areas in S960QL High Strength Steel', *Metals*, 9, 1226, 2019, https://doi.org/10.3390/met9111226.

[12] M-M. RAN, F-F. SUN, G-Q. LI, A. KANVINDE, Y-B. WANG, R.Y. XIAO: 'Experimental study on the behavior of mismatched butt welded joints of high strength steel', *Journal of Constructional Steel Research*, 153, pp. 196-208, 2019, https://doi.org/10.1016/j.jcsr.2018.10.003.

[13] C. RODRÍGUEZ, J.G. CABEZAS, E. CÁRDENAS, F.J. BELZUNCE, C. BETEGÓN: 'Mechanical Properties Characterization of Heat-Affected Zone Using the Small Punch Test: Use of the small punch test for the mechanical characterization of small areas such as the different zones that characterize the HAZ showed promise', *Welding Journal, 88, 2009.*

[14] J. GIGAX, A. TORREZ, Q. MCCULLOCH, H. KIM, S. MALOY, N. LI: 'Sizing up mechanical testing: Comparison of microscale and mesoscale mechanical testing techniques on a FeCrAl welded tube', *Journal of Materials Research*, 35(20), 2817-2830, 2020. doi:10.1557/jmr.2020.195

[15] P.A. STATHERS, A.K. HELLIER, R.P. HARRISON, M.I. RIPLEY, J NORRISH: 'Hardness-tensile property relationships for HAZ in 6061-T651 aluminum', *Faculty of Engineering and Information Sciences,* Papers: Part A. 2846, 2014, https://ro.uow.edu.au/eispapers/2846.

[16] L. ZHANG, W. HARRISON, M.A. YAR, S.G.R. BROWN, N.P. LAVERY: 'The development of miniature tensile specimens with non-standard aspect and slimness ratios for rapid alloy prototyping processes', *Journal of Materials Research and Technology*, Volume 15, pp. 1830-1843, 2021, https://doi.org/10.1016/j.jmrt.2021.09.029.

[17] T.W. CLYNE, J.E. CAMPBELL, M. BURLEY, J. DEAN: 'Profilometry-Based Inverse Finite Element Method Indentation Plastometry', *Advanced Engineering Materials*, vol. 23, 9, 2100437, 2021, https://doi.org/10.1002/adem.202100437.

[18] W. GU, J. CAMPBELL, Y. TANG, H. SAFAIE ET AL.: 'Indentation Plastometry of Welds', *Advanced Engineering Materials*, 2101645, 2022, https://doi.org/10.1002/adem.202101645

[19] J.E. CAMPBELL, M. GAISER-PORTER, W. GU, S. OOI ET AL.: 'Indentation Plastometry of Very Hard Metals', *Advanced Engineering Materials,* 2101398, 2022, https://doi.org/10.1002/adem.202101398

[20] ABAQUS: *Abaqus/Explicit User's Manuals,* Version 6.11, Dassault Systèmes Simulia Corp. Providence, RI, USA, 2011.

[21] Y. CHO, C. LEE, J.-J. YEE, D.-K. KIM: 'Modeling of Ductile Fracture for SS275 Structural Steel Sheets', *Appl. Sci.*, 11, 5392, 2021, https://doi.org/10.3390/app11125392.

[22] S. YAN, X. ZHAO, A. WU: 'Ductile Fracture Simulation of Constructional Steels Based on Yield to-Fracture Stress–Strain Relationship and Micromechanism-Based Fracture Criterion',

Journal of Structural Engineering, Vol 144, Issue 3, 2018, https://doi.org/10.1061/(ASCE)ST.1943 541X.0001970.

[23] F. SHEN, S. MÜNSTERMANN, J. LIAN: ‘Investigation on the ductile fracture of high-strength pipeline steels using a partial anisotropic damage mechanics model’, *Engineering Fracture Mechanics,* Vol 227, 2020, https://doi.org/10.1016/j.engfracmech.2020.106900.

[24] V.N. VAN DO: ‘The Behavior of Ductile Damage Model on Steel Structure Failure’, *Procedia Engineering,* Vol 142, 26-33, 2016, https://doi.org/10.1016/j.proeng.2016.02.009.

[25] C. LI, D.E, N. YI: ‘Analysis on fracture initiation and fracture angle in ductile sheet metal under uniaxial tension by experiments and finite element simulations’, *Journal of Materials Research*, *31*(24), 3991-3999, 2016, doi:10.1557/jmr.2016.412.